

Electrochemical polymerization of 7-methylthionaphthene-indole

G. CASALBORE-MICELI, G. BEGGIATO, P. G. DI MARCO, A. GERI, G. GIRO

Istituto di Fotochimica e Radiazioni d'Alta Energia (FRAE) del Consiglio Nazionale delle Ricerche, Via de'Castagnoli 1, 40126 Bologna, Italy

Received 15 June 1989; revised 15 August 1989

The effect of the methyl substituent in position 7 on the electrochemical polymerization of 7-methylthionaphthene-indole (7-methyl[1]benzothieno[3,2-b]indole; MTNI) was investigated. Acid-base equilibria involving the heterocyclic nitrogen were observed. The electrolytic synthesis of oxidized poly-MTNI is a process controlled by a protonation-deprotonation mechanism. The electrical conductivity of this material was measured.

1. Introduction

Defining the coupling sites of the monomer units is one of the critical steps in the structural characterization of polymers obtained by electrochemical oxidation of heterocycles. This problem is obviously more complex when the monomer is a large molecule with several potential sites. For small monomers such as pyrrole and thiophene, the determination of the active positions in the molecule was very important to foresee and study the molecular structure and the electrical features of the resulting oligomers or polymers. In the case of carbazole the sites of the radical cations responsible for coupling were identified as positions 3 and 9 (Fig. 1) [1-4].

In previous works [5-10] we studied thionaphthene-indole ([1]benzothieno[3,2-b]indole; TNI) (Fig. 1) and some of its derivatives. In these cases mass spectrometry (MS) measurements and theoretical calculations did not allow the coupling sites to be determined definitively. For this reason we focused our interest on 7-methyl-TNI (MTNI), because position 7, equivalent with respect to N to position 3 of carbazole, can be considered very reacting in the radical cation coupling leading to quinoid dication structures. Besides, hydrogen in position 10 allowed us to study acid-base equilibria, which are active in the oxidation process of N-heterocycles, as suggested in [2, 9].

2. Experimental details

TNI, from which MTNI was obtained, was prepared as reported in [10]. Methylation of position 7 was performed with methyl iodide in dimethylformamide and sodium hydride. The product was purified by chromatography and characterized by nuclear magnetic resonance (NMR) and MS.

Purification of the solvent (methylene chloride; Merck 'pro analysi') and of the supporting electrolyte (tetrabutylammonium perchlorate (TBAP); Fluka 'purum') and a description of the apparatus and elec-

trolytic cell used for voltammetry and electrolyses were described elsewhere. As reference a saturated calomel electrode (SCE) was used, to which all potentials are referred in this paper. The platinum counter-electrode was separated from the working electrode compartment by a sintered glass disc. The working electrode was a platinum microelectrode (1.92 mm²) for voltammetry and a 1 cm² platinum plate or a 1.5 cm × 1.5 cm glass plate coated with indium tin oxide (ITO) for electrolyses. All experiments were carried out at room temperature (about 22°C) under nitrogen atmosphere. Ultra violet-visible spectra were recorded with a Perkin-Elmer Lambda 5 instrument; to extend the spectral analysis to the near-infrared (NIR) region a Perkin-Elmer Lambda 9 spectrophotometer was also used.

The electrical conductivity of poly-MTNI was measured on compressed (3 t) 0.196 cm² pellets with a Keithley 195A digital multimeter.

The results of the elemental analysis of the polymer were the following: C 54.15%, H 3.10%, O 18.44%, S 8.71% Cl 6.84%.

3. Results and discussion

3.1. Electrochemical experiments

MTNI, as well as the analogous compounds of the TNI family, shows two anodic waves: at +1 V (a potential very close to that at which most of the N-heterocycles are oxidized) and at a potential more anodic than +1.4 V (Figs 2a and b). The former wave does not show evident differences with respect to analogous molecules: it is monoelectronic and the slope of its logarithmic plot (E against $\log [(i_1 - i)/i]$) is 70 mV. However, in this case a small post-wave, observed for other compounds [9] and attributed to acid-base equilibria involving protons, produced by the electrode reactions and heterocycle nitrogen was not detectable.

For the other TNI derivatives the second wave was

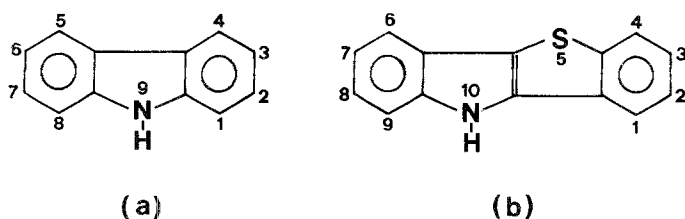


Fig. 1. (a) Carbazole and (b) thionaphthene-indole (TNI).

not completely visible, because at +1.7/+1.8 V, before reaching the limiting current, electrode passivation or solvent discharge occurred. For MTNI this wave was fully visible: with 1.04×10^{-4} M MTNI the measured half-wave potential was +1.58 V. It was also irreversible, as the slope of the logarithmic plot (74 mV), in spite of the high electron consumption of the process, and the absence, in cyclic voltammetry (CV), of the cathodic peak corresponding to the anodic one, clearly suggest.

At the lowest MTNI concentrations (1×10^{-3} – 5×10^{-4} M) the ratio between the first and the second wave was 1:3. By increasing the concentration this ratio decreased due to electrode passivation.

It is worthy of note that the second wave was also observed in the voltammograms of phenothiazine [11], a heterocycle with both S and N, and was attributed to bioxidation of the monomer. Therefore, in our case the overall process connected with this wave, taking into account the electron consumption of the process, could be the formation of the dication, promptly followed by coupling between dications with production of acidity and oxidation of the oligomer so obtained. The coupling between dications should be in competition with the reaction between dications and solvent.

The CV of MTNI from –1 to +1.4 V (Fig. 2c) shows an anodic peak at +1.05 V, with the corresponding cathodic peak at +0.97 V. The higher ratio between the cathodic and anodic peak decreases, as

shown in Table 1, as the sweep rate increases, bringing to light the kinetics subsequent to the radical cation formation.

The CV from –1 to +1.8 V (Fig. 2d) shows, besides the peak at +1.05 V, a second peak at +1.66 V, which is more than twice the height of the first and corresponds to the most anodic voltammetric wave. This peak is fully irreversible; however, a series of small reduction peaks was observed at 0, +0.2, +0.4 and +0.8 V, which could be due to the reduction of H^+ and of oligomers oxidized and/or protonated. The CV extended to +1.8 V shows that the primary product associated with the second peak is extremely reactive and strongly supports the dication hypothesis. The parameters of the DLRVs and CVs are shown in Table 1.

Preparative electrolyses were performed at the plateau potentials of both anodic waves of MTNI. They are characterized by an initial decrease of current density, which remains at a constant low level for a long time. This behaviour, similar to that shown by the analogous compounds already studied [2], suggests equilibria between MTNI and electrolysis products: H^+ and non-oxidized N-heterocycles. These equilibria, described for other cases [12], make polymers like this similar to polyanilines, the redox steps of which frequently coincide with protonation–deprotonation reactions.

The consumption of electrons per monomer, which in all cases is reached when the current is about 10% of the initial value, is certainly > 2 , being about 2.6 for the highest concentrations of MTNI. The end of electrolysis probably occurs after days with a progressive increase of the molecular weight of the oligomers. The electrolytic process evidently consists of alternate reactions of protonation–deprotonation–coupling; the protonation–deprotonation equilibria involving the heterocycle nitrogen of the neutral structures are determining steps. Oxidized oligomers with more than two monomer units, insoluble in methylene chloride* were not observed by electrolysing 5×10^{-4} M MTNI solutions whereas at intermediate concentrations (1 – 3×10^{-3} M) small amounts of these products were formed, their yield increasing when 5×10^{-3} M solutions were electrolysed.

Meaningful differences in the voltammetric and spectrophotometric patterns were not detectable by oxidizing on the first (+1.2 V) and second (+1.7 V) wave. The only difference was the polymer yield, which was higher (54%) at +1.2 V than at +1.7 V

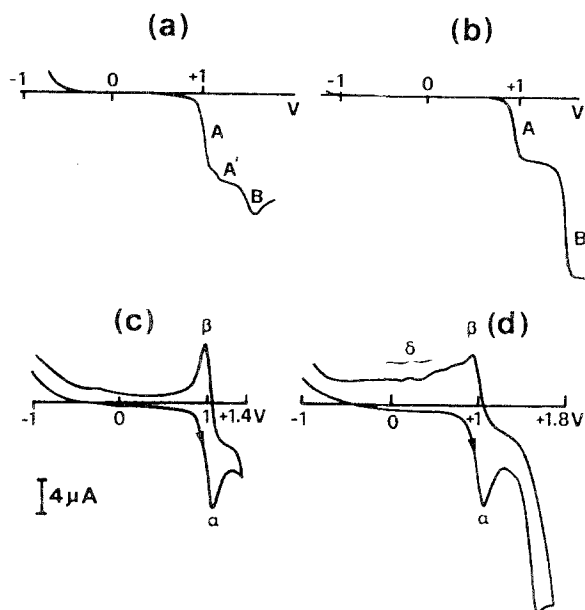


Fig. 2. DLRV of (a) 0.99×10^{-3} M TNI and (b) 1.04×10^{-3} M MTNI (0.1 M TBAP) in methylene chloride. CV of 1.04×10^{-3} M MTNI (0.1 M TBAP) in methylene chloride (sweep rate 100 mV s^{-1}); (c) from –1 to +1.4 V and (d) from –1 to +1.8 V.

* In [6, 9] it was demonstrated that the oxidized dimers of N-allyl-TNI and TNI are soluble in methylene chloride.

Table 1. Diffusion layer renewal voltammetry (DLRV) and cyclic voltammetry (CV) parameters for different MTNI concentrations in methylene chloride (supporting electrolyte: 0.1 M TBAP)

DRLV parameters				
MTNI concentration ($M \times 10^3$)	Waves			
	$E_{1/2}$ (V)	i_l (μA)	$E_{1/2}$ (V)	i_l (μA)
0.42	0.96	3.3	1.53	10.4
1.04	1.00	7.0	1.58	20
3.00	0.99	20.8	1.61	42
5.05	1.02	43.2	—	—
CV parameters ($v = 100 \text{ mV s}^{-1}$)				
MTNI concentration ($M \times 10^3$)	Peaks			
	E_p (V)	i_p (μA)	E_p (V)	i_p (μA)
0.42	1.12	4.2	0.92	3.0
1.04	1.07	12.0	0.97	7.4
2.71	1.09	28.4	0.94	16.8
5.05	1.03	68.8	0.91	40.8
CV parameters of $5.05 \times 10^{-3} \text{ M MTNI}$				
	v (mV s^{-1})			
	20	50	100	200
i_{pc}/i_{pa}	0.31	0.44	0.59	0.63
i_{pa}/\sqrt{v}	7.87	7.24	6.88	6.56

i_l , limiting current (μA); i_{pa} , anodic peak current (μA); i_{pc} , cathodic peak current (μA); v , sweep rate (mV s^{-1}).

(38%). This can be justified by the higher probability of side reactions involving the solvent at more anodic potentials. The results obtained by oxidizing MTNI at +1.2 and +1.7 V demonstrate clearly that the products of the electrolysis, even if the reaction mechanism is different, are very similar or identical. The low oligomer yield at the lowest monomer concentrations can be explained by the dominant formation of products of low molecular weight, like soluble oxidized or neutral protonated dimers owing to minor concentrations of reacting species. The high yields of oxidized polymers of TNI [7] and MTNI suggest that these two compounds have similar polymerization reactivities.

In [6] positions 7 and 10 were indicated as the most probable coupling sites of the radical cations of TNI and derivatives. This hypothesis was supported by the following observations.

(1) The TNI derivatives show analogies with the carbazoles, which dimerize in positions corresponding to position 7 and position 10 of TNI.

(2) Oxidized heterocycle oligomers with bipolaron units or also dication dimers with monomer moieties connected in positions 7 or 10 are strongly stabilized by quinoid structures.

(3) N-allyl-TNI (ATNI), a molecule with position 7 free but position 10 unavailable, electrolysed on the first anodic wave only gives dication dimers, whereas TNI, with both positions free, also gives oxidized oligomers according to the experimental conditions [7].

Theoretical calculations [8] did not give substantial support to these observations. In fact, the spin density map does not show meaningful differences among all positions where coupling is possible. Thus, this work demonstrates that, position 7 being unavailable, the second reactive point, besides position 10 (N atom), is to be found in position 6, 8 or 9 of the benzene ring adjacent to N or in positions of the benzene ring adjacent to S. In the first ring only position 9 could be stabilized by quinoid structures in dication dimers or bipolaron oligomers. However, this position seems to be sterically hindered for the second coupling, as the behaviour of phenothiazine suggests [13]. The position of this molecule, equivalent to position 9 of MTNI, was utilized to give dimers but the cations of the resulting products, owing to lack of coplanarity, do not show conjugation between the two moieties of the molecule, which spectrally behave like independent units.

From all of these considerations we can conclude that, unlike small molecules such as pyrrole or thiophene, the radical cations of TNI and derivatives, owing to their molecular size, have several almost equivalent coupling sites. This conclusion is also supported by calculations [14] which show that, in the polymerization of pyrrole and thiophene, as the molecular size increases, the coupling stereospecificity of the radical cations decreases.

As reported above, the electrolysis of MTNI, both on the first and on the second anodic wave, produces

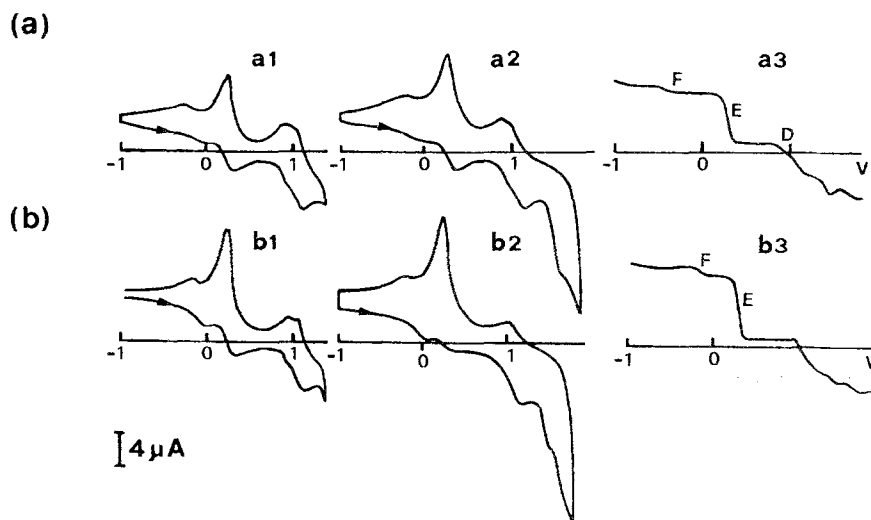


Fig. 3. CV from (a1) -1 to $+1.4$ V and from (a2) -1 to $+1.8$ V (sweep rate 100 mVs^{-1}), and (a3) DRLV of $1.04 \times 10^{-3} \text{ M}$ MTNI in methylene chloride (0.1 M TBAP), electrolysed at $+1.7$ V, after the flow of 1.7 electrons per monomer. (b1) CV from -1 to $+1.4$ V and from (b2) -1 to $+1.8$ V (sweep rate 100 mVs^{-1}), and (b3) DRLV of $1.04 \times 10^{-3} \text{ M}$ MTNI in methylene chloride (0.1 M TBAP), electrolysed at $+1.2$ V, after the flow of 2.1 electrons per monomer.

an oxidized oligomer at higher monomer concentrations, whereas at low concentrations a blue-violet solution is obtained, the DRLV and CV of which are shown in Fig. 3. In all of these experiments three cathodic waves at $+0.9$, $+0.3$ and -0.4 V and a series of anodic waves, from $+0.9$ to $+1.5$ V (beyond this potential passivation occurs) were observed. The cathodic waves are due to reduction of oxidized dimers, H^+ and protonated neutral oligomers, as suggested and discussed in [9, 10]. Anyway, it is important to underline the following experimental results.

(1) The reduction wave of H^+ in methylene chloride is at $+0.22$ V (HClO_4 $4.7 \times 10^{-3} \text{ M}$).

(2) The cathodic wave at -0.4 V decreases gradually to zero with time after the end of the electrolysis, but the total height of the cathodic waves remains almost unchanged due to the contemporary increase of the wave at $+0.3$ V.

(3) During the electrolyses the methylene chloride solution turns gradually from blue to green and the cathodic wave at $+0.3$ V becomes the main one, so that it remains practically the only wave for long electrolysis times. The green solution becomes yellow if it is shaken with aqueous NaOH but it turns green again after acidification with HCl.

(4) The height of the cathodic wave at $+0.9$ V is proportional to the spectral absorbance at 580 nm and goes rapidly to zero after the end of the electrolysis (Fig. 4).

3.2. Oxidation mechanism

According to the above considerations, the oxidation mechanism of MTNI can be described by the reactions of Scheme 1. In this scheme, besides the reaction products between radicals and solvent, the reducible dimers can be subdivided into three different classes: neutral protonated dimers (3', 4' and 5'), oxidized dimers, which cannot be reduced by deprotonation (8, 12 and 13), and oxidized dimers, which can be reduced by deprotonation (6, 9, 10 and 11).

Oxidized radical monomers may also exist, but they should be very unstable in methylene chloride, because the primary products obtained by pulse radiolysis oxidation of TNIs live for microseconds [8] and, by reacting with the solvent, give products which do not absorb in the visible region.

The CV of MTNI, besides the reduction peak of the primary radical cation, the height of which depends on the sweep rate, does not show other notable cathodic peaks in the range $+0.9$ to $+1.8$ V. Referring to

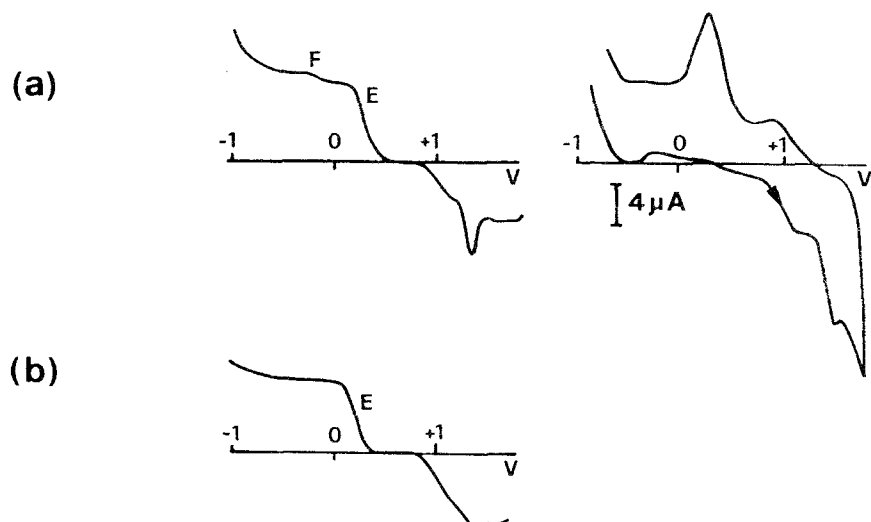
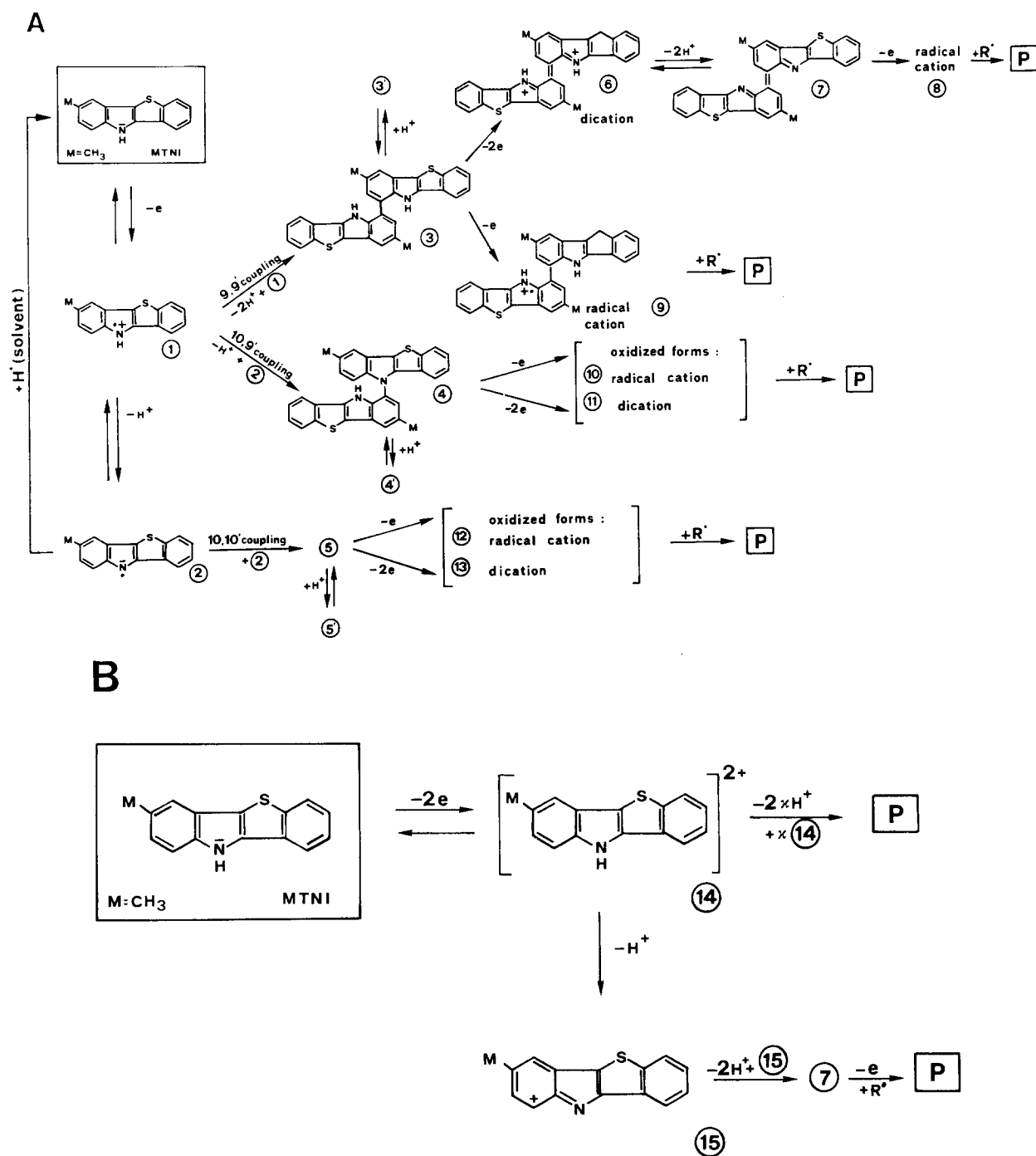


Fig. 4. (a) DRLV and CV (sweep rate 100 mVs^{-1}) of $1.04 \times 10^{-3} \text{ M}$ MTNI in methylene chloride (0.1 M TBAP) 16 h after the end of electrolysis at $+1.2$ V (flow of 2.1 electrons per monomer). (b) DRLV of $3 \times 10^{-3} \text{ M}$ MTNI in methylene chloride (0.1 M TBAP) 62 h after the end of electrolysis at $+1.7$ V (flow of +1.9 electrons per monomer).



Scheme 1. Electrolytic oxidation mechanism of MTNI electrolysed (A) on the first (+1.2V) and (B) on the second (+1.7V) wave. P, polymer.

Scheme 1, the cathodic wave at +0.9V could be associated with the reduction of oxidized dimers (8, 12 and 13), without protonation equilibria, the cathodic wave at +0.3V with the reduction of H^+ and of neutral protonated compounds involved in acid-base equilibrium and the cathodic wave at $-0.4V$ with the dimeric structures (like 6), which deprotonate slowly to 7 and H^+ . Alternatively, taking into account TNI, the cathodic wave at +0.9V could be attributed to reduction of radical compounds like 8, and the other two cathodic waves should be associated with reduction of H^+ and other dimeric species, protonated or bearing positive charges.

The cathodic waves connected with reduction of the

soluble compounds produced by oxidation of TNI derivatives are difficult to explain; however, the main process is reduction of H^+ , free or linked to the heterocycle nitrogen of the soluble species.

The anodic waves which appear after oxidative electrolysis of MTNI are due mainly to oxidation of condensed and protonated neutral compounds. The oxidation potential of these compounds is more anodic than that of the monomer, owing to the protonation of the heterocycle N and/or because the position of the coupling does not allow a planar structure to be obtained.

After the end of electrolysis these waves increase a little with time, owing to both deprotonation of

species like **6** and subsequent acid–base equilibrium of the products, and to spontaneous reduction of the species **8** and **12**. As expected, by reduction on the plateau (-0.3 V) of the cathodic wave at $+0.3$ V due to electrooxidation of MTNI, a decrease of all cathodic waves and an increase of the anodic ones is observed, and the absorbance in the visible region decreases.

As pointed out previously, the CVs are not meaningfully different after electrolysis on the plateau of the first and the second anodic wave (Fig. 3). By sweeping from -1 to $+1.4$ V, two anodic peaks in the range $+0.9$ to $+1.5$ V and the corresponding cathodic peaks were observed (the couple of peaks at $+0.95/+0.92$ V could correspond to the wave at $+0.9$ V). A triangular peak at about $+0.25$ V, corresponding to the wave at -0.3 V were also observed; they were not reversible and only one small anodic peak at about $+0.3$ V remained after a second sweep. The CV from -1 to $+1.8$ V did not differ appreciably from that limited to $+1.4$ V, apart from a peak at about $+1.56$ V, probably due to formation of dication in condensed structures (dimer \rightarrow dication dimer).

3.3. Absorption spectra

Understanding of the reaction mechanism of MTNI electrooxidation was facilitated by analysis of the absorption spectra recorded during the experiments. The spectrum of MTNI, shown in Fig. 5, is very similar to that of TNI. After electrolyses, both on the first and on the second anodic wave, a decrease of the ultraviolet absorption and the appearance of new

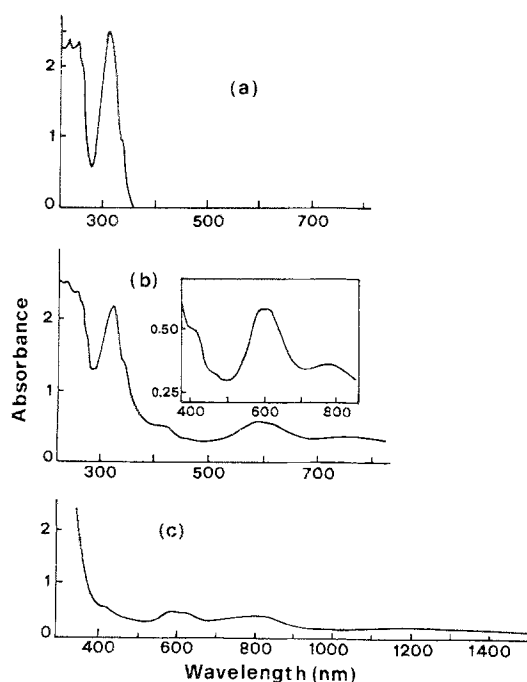


Fig. 5. Absorption spectra of (a) 1.04×10^{-3} M MTNI in methylene chloride, (b) 2.7×10^{-3} M MTNI in methylene chloride electrolysed at $+1.2$ V (flow of 1.9 electrons per monomer), (c) 5.05×10^{-3} M MTNI in methylene chloride electrolysed at $+1.2$ V (flow of 2.6 electrons per monomer); optical path 0.1 cm. Inset: part of (b) enlarged.

smaller bands in the visible and near-infrared regions were observed in both cases. In particular, the spectrum was characterized by maxima at about 580, 600, 800, 1200 and 1600 nm and two shoulders at 400–420 and 470–480 nm. The bands at 580 nm, 800 nm and in the near-infrared, proportionally higher for diluted solutions, are due to oxidized dimers. Owing to the coupling of the oxidized species in solution, these bands decrease with time, after the end of electrolysis, as well as the cathodic wave at -0.9 V. The shoulder at 400–420 nm is due to neutral oligomers and does not depend on their protonation, because, by alkalization, the absorption remains unchanged at this wavelength, whereas all visible bands disappear.

By comparison of the spectra of MTNI and TNI, electrolysed under the same conditions, high absorbances around 500 and 800 nm were observed for high concentrations of TNI, whereas for MTNI the absorbances in the visible region were always quite low. The strong methyl effect can be explained either by the greater proton affinity of the heterocycle nitrogen, due to the electron-donating effect of the methyl substituent, which makes the ratio higher in the electrolysed samples between protonated neutral dimers and oxidized dimers, or by different coupling sites of the radical cations, with consequent changes of dimer molar absorbance due to differences of charge conjugation.

3.4. Solid-state characterization

The oxidized solid polymer was obtained on an ITO electrode. The spectrum of the polymer layer (Fig. 6) showed maxima at 608, 800 and about 1500 nm, in good agreement with the bands attributed in solution to oxidized dimers; by increasing the film thickness, the absorbance increases all over the visible–near-infrared region and the spectrum becomes less structured, because the system tends to the metal-like state.

From elemental analysis the formula of the oxidized polymer is $(C_{16.58}H_{11.3}N_{1.12}S_1) 0.71(ClO_{5.97})$. Taking into account the presence of water, as suggested by the high H and O percentages and observed in other cases [5], and of small traces of supporting electrolyte, the formula of the oxidized product may be $(C_{15}H_5N_{1.03}S_1) 0.62(ClO_4) 1.4H_2O 0.1TBAP$, in very good agreement with the theoretical composition, except for a negative difference in the hydrogen amount. Referring to the formula above, the yield of the product was 54% for electrolyses at $+1.2$ V and 38% at $+1.7$ V, not too different from that already obtained with TNI (44%).

The electrical conductivity of the oxidized polymer, measured as reported in Section 2, was $2.8 \times 10^{-4} \text{ S cm}^{-1}$.

4. Conclusions

Substituting hydrogen in position 7 of TNI with a methyl group does not influence the electrochemical formation of an oxidized polymer. This observation, which does not agree with a preferential coupling in

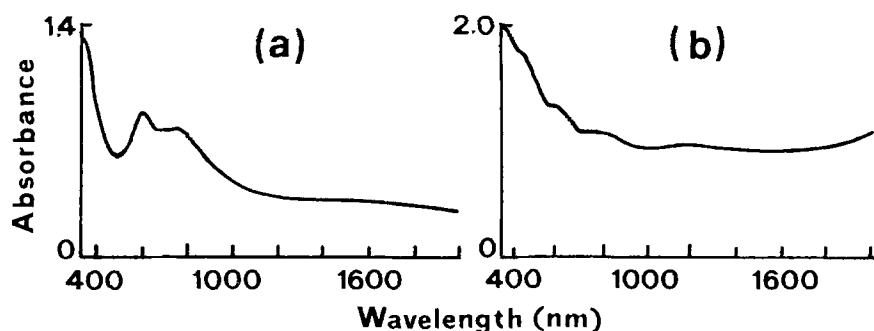


Fig. 6. Absorption spectra of poly(MTNI) obtained from 5.05×10^{-3} M MTNI in methylene chloride electrolysed at +1.2 V (flow of 2 electrons per monomer), after further flow of (a) 0.2 C and (b) 0.46 C (absorbance of ITO glass subtracted).

position 7, supports the conclusion that, in the cations of TNI derivatives, several sites are equally reactive as far as coupling is concerned, according to the spin density map, as discussed in [8].

Methylation in position 7 shifts the anodic waves of the voltammetric pattern of TNI towards less-anodic potentials. The second wave is shifted more than the first. This fact, which allowed the second wave to be readily investigated, can be explained by assuming that the second wave is associated with an oxidation process involving an orbital delocalized all over the molecule, whereas the first wave concerns an orbital mainly centered on the N atom and influenced less by the electron-donating effect of the methyl group in position 7. Molecules with heterocycle nitrogen show an anodic wave at potentials close to those observed for the TNI family.

The oxidation process on the second wave is nearly trielectronic. Then, the most obvious deduction is that, by electrolysis on this wave, dications are formed, which interact rapidly giving oxidized polymer. Indeed, the second wave is fully irreversible, as shown by CV experiments. However, by oxidizing on this wave, large differences either in the polymer production or in the voltammetric and spectrophotometric patterns were not observed with respect to electrolysis on the first wave. This may be due to electrode passivation, which may occur at these potentials and make the processes different in electrolyses and voltammetry, respectively, or to accumulation during the electrolysis of large numbers of protons responsible for acid-base equilibria of N-heterocycle compounds. These acid-base equilibria became evident in this work. Indeed, the electrolytic synthesis of oxidized poly-MTNI is a slow process, controlled by a protonation-deprotonation mechanism, and therefore it may last quite a few hours.

Thin layers of poly-MTNI show a structured visible-

near-infrared spectrum; the absorbance becomes nearly uniform all over the spectrum (metal-like behaviour) for relatively thick films. This polymer shows a dark conductivity of $2.8 \times 10^{-4} \text{ S cm}^{-1}$.

Acknowledgements

We thank Mr G. Gubellini for drawing the figures and Mr. L. Minghetti for technical assistance. This work was supported by Progetto Finalizzato 'Nuovi Materiali' of Consiglio Nazionale delle Ricerche.

References

- [1] J. F. Ambrose and R. F. Nelson, *J. Electrochem. Soc.* **115** (1963) 1159.
- [2] A. Desbone-Monvernay, P. C. Lacaze and J. E. Dubois, *J. Electroanal. Chem.* **129** (1981) 229.
- [3] F. J. Davis, H. Block and R. G. Compton, *J. Chem. Soc., Chem. Commun.* (1984) 890.
- [4] C. I. Simionescu, M. Grovu-Ivanouiu and M. Grigoras, *Eur. Polym. J.* **22** (1986) 71.
- [5] G. Casalbore-Miceli, G. Beggiato, P. G. Di Marco, S. S. Emmi, G. Giro and B. Righetti, *Synth. Met.* **15** (1986) 1.
- [6] G. Casalbore-Miceli, G. Beggiato, S. Daolio, P. G. Di Marco, S. S. Emmi and G. Giro, *Ann. Chim. (Rome)* **77** (1987) 609.
- [7] G. Casalbore-Miceli, G. Beggiato, S. Daolio, P. G. Di Marco, S. S. Emmi and G. Giro, *J. Appl. Electrochem.* **17** (1987) 1111.
- [8] G. Beggiato, G. Casalbore-Miceli, S. S. Emmi, P. G. Di Marco, G. Giro and G. Poggi, *Bull. Soc. Chim.* (1987) 301.
- [9] G. Casalbore-Miceli, G. Beggiato, S. S. Emmi, A. Geri, B. Righetti and S. Daoli, *J. Chem. Soc., Perkin Trans. II* (1988) 1231.
- [10] G. Casalbore-Miceli, G. Beggiato, S. S. Emmi, A. Geri, S. Daolio, *J. Appl. Electrochem.* **18** (1988) 885.
- [11] G. Cauquis, A. Deronzier, J. L. Lepage and D. Serve, *Bull. Soc. Chim.* (1977) 304.
- [12] G. Zotti, S. Catarin and N. Comisso, *J. Electroanal. Chem.* **235** (1987) 259.
- [13] C. Cauquis, A. Deronzier, J. L. Lepage and D. Serve, *Bull. Soc. Chim.* (1977) 304.
- [14] R. J. Waltman and J. Barogn, *Tetrahedron* **40** (1984) 3963.